# A COMPARISON OF QUANTITATIVE ACOUSTIC, MAGNETIC AND PERMEABILITY ANISOTROPY MEASUREMENTS ON A NORTH SEA CAPROCK

[†]Muhammad Arif, [†]David K. Potter, [†]Ross Bishop, *Norbert Schleifer and [+]Stefano Pruno

[†]Department of Physics, University of Alberta, Edmonton, Canada

*Wintershall Holding GmbH, Rechterner Str. 2, 49406 Barnstorf, Germany

[+]Weatherford Laboratories, Stavanger, Norway

*This paper was prepared for presentation at the International Symposium of the Society of Core Analysts held in Napa Valley, California, USA, 16-19 September, 2013*

## ABSTRACT

Caprocks or seals are important components of a reservoir system, and are generally characterised by low permeability values. It is rare, however, that petrophysical measurements on caprock core material specify the direction in which the measurements such as permeability or acoustic velocity (which are generally one dimensional) are taken. It is therefore often assumed that the caprocks are isotropic. However, the effectiveness of a caprock may depend in part on how anisotropic that caprock is and the orientation of the principal anisotropy axes. The purpose of the present paper was to take an unconventional approach and compare and quantify the magnitude and orientation of the acoustic, magnetic and permeability anisotropy of a North Sea caprock. The magnetic anisotropy involved anisotropy of magnetic susceptibility (AMS) and anisotropy of isothermal remanent magnetization (AIRM). The samples studied showed significant acoustic, magnetic and permeability anisotropy parallel and perpendicular to the observed petrofabric. Comparisons between the magnitudes and orientations of the acoustic, magnetic and permeability anisotropies could potentially allow estimates of one type of anisotropic property from measurements of a different anisotropic property. In the samples studied all the techniques gave consistent results, with maximum acoustic velocity, permeability, AMS and AIRM axes being parallel to the observed petrofabric (the horizontal axis in these cases).

## INTRODUCTION

Our study was motivated by the idea that the degree and orientation of the anisotropic properties of a caprock might be an important factor in determining the efficiency of the caprock. Anisotropic properties of caprocks have been rarely studied. The objective of the present study was to quantify and compare acoustic anisotropy (both *p*- and *s*-wave anisotropies), anisotropy of magnetic susceptibility (AMS), anisotropy of magnetic

remanence (AMR) and permeability anisotropy. We studied in detail the anisotropic properties of two core plug samples from the same caprock or seal (a siltstone lithology) from a North Sea reservoir. One plug was cut in the horizontal direction (sample 4H) and the other in the vertical direction (sample 2V). Part of each core plug was used for acoustic and permeability anisotropy studies, and another part of each core plug was used for magnetic anisotropy studies (Figure 1).

We first undertook *p*-wave and permeability measurements on horizontal and vertical plugs that were closely parallel and perpendicular to the observed petrofabrics. We also utilized *s*-wave splitting so that we could get some indication of anisotropy from two measurements of the *s*-wave velocity (using *s*-waves polarized in two orthogonal directions) in a single plug, rather than needing to use 2 plugs cut in two orthogonal directions. The acoustic measurements were undertaken at a variety of hydrostatic pressures from ambient to typical reservoir (overburden) pressures, and the *p*-wave and *s*-wave velocities in the different directions as a function of pressure were determined. This acoustic analysis alone doesn't give one the full 3D anisotropy or the orientation of the 3 principal anisotropy axes. Therefore we also undertook anisotropy of magnetic susceptibility (AMS) measurements, which allows one to rapidly determine the complete 3D anisotropy ellipsoid using just one core plug, by spinning the sample about 3 orthogonal axes in an anisotropy delineator. This technique gives the orientation and magnitude of the 3 principal magnetic susceptibility axes. An additional novel magnetic anisotropy technique, anisotropy of isothermal remanent magnetization (AIRM), was also employed to determine the anisotropy of the fine ferrimagnetic particles (generally iron oxides) in the core plugs.

## METHODS

### 1. Visible Petrofabric

Mineral alignments (especially clays) were observed in the samples with the unaided eye, and with a hand lens, and also via thin sections. This visible petrofabric was compared with the other quantitative anisotropy techniques. X-ray diffraction was also undertaken to determine the main minerals in the samples.

### 2. Acoustic Anisotropy

A pulse transmission method was used to make the acoustic measurements. Piezoelectric ceramic transducers (made of lead zirconate titanate from Omega Piezo Technologies Inc) were used to generate the *p*- and *s*-waves. The polarization of the piezoelectric ceramic transducers determines the vibration mode. The axial polarization causes a compressional/tensional vibration mode and generates a compressional wave or *p*-wave, whereas the lateral polarization causes a shear vibration mode and generates a shear wave or *s*-wave. The *s*-wave piezoelectric ceramic is placed on the top of an aluminum buffer. The *p*-wave piezoelectric ceramic is placed on the top of the *s*-wave piezoelectric ceramic, but separated by an electrode made of copper foil (Bakhorji, 2010). The core plug samples used for the acoustic measurements were 2.5cm in diameter but slightly

different lengths (merely due the available length of each core sample). The horizontal plug 4H was 5.2 cm long and the vertical plug 2V 4.05 cm long. The end faces of each plug were polished to ensure good contact with the transducers. Each plug was then placed into securely fitting reinforced Tygon$^{TM}$ plastic tubing. The transmitter transducer was attached to one end of the sample inside the plastic tubing and the receiver transducer to the other end. The receiver and transmitter transducers were aligned to ensure proper polarization of the shear wave ceramic transducers. The experimental system consisted of a pressure vessel, a pulse generator, and a digital oscilloscope. The maximum hydrostatic pressure used in this study was 40 MPa, which was estimated to be the maximum in situ overburden pressure of these North Sea caprocks. The pulse generator (Panametrics, model 5800 PR) pulses the piezoelectric transducers with a fast-rising 200 V square wave, which results in the propagation of the wave through the sample and was recorded by a digital oscilloscope. The acoustic frequency was 1 MHz. The oscilloscope recorded the signal in time intervals of 2-10ns and gave a final waveform as a stack of 256 traces to minimize random noise. The waveforms were transferred to a computer system for later transit time calculation (using the methodology of Hemsing, 2007 and Bakhorji, 2010). The hydrostatic pressure was raised up in increments of 5MPa on both the up cycle (increasing pressure) and down cycle (decreasing pressure). The *p*-wave velocity at each pressure increment was determined along the long axis (z axis) of each of the horizontal (4H) and vertical (2V) core plugs (indicated by the red arrows in Figure 2). The *s*-wave velocity at each pressure increment was determined along the x and y axes (indicated by the blue and green arrows respectively in Figure 2) of each core plug.

**3. Anisotropy of Magnetic Susceptibility (AMS)**

Low field anisotropy of magnetic susceptibility (AMS) only requires 1 core plug to compute the 3D anisotropy. We used a Molspin anisotropy delineator, which spins the sample about 3 orthogonal axes (x, y and z) in turn and computes the anisotropy in the respective planes (yz, zx and xy). By adding the bulk magnetic susceptibility along one axis (z axis), using a Molspin magnetic susceptibility bridge, a complete 3D anisotropy ellipsoid can be computed. An AMS measurement of this type, together with the bulk magnetic susceptibility reading, can be undertaken in around two minutes. The technique is very sensitive and can measure anisotropies to about 1 part in 10,000, unless the bulk magnetic susceptibility signal is very low. This degree of sensitivity is considerably better than permeability anisotropy or acoustic anisotropy techniques. Low field AMS gives the sum of the anisotropies of all the mineral components in the sample, so anisotropies due to different mineral components cannot be separated. AMS is also dependent upon ferrimagnetic particle size. Uniaxial stable single-domain particles have a minimum magnetic susceptibility along their long axis, whilst larger multidomain particles have a maximum magnetic susceptibility along their long axis (Potter, 2004).

**4. Anisotropy of Magnetic Remanence (AMR)**

Anisotropy of magnetic remanence (AMR) techniques measure the anisotropy of the remanence carrying minerals only (generally the ferimagnetic minerals). These are

generally iron oxides, which can sometimes block pores and influence permeability. Anisotropy of isothermal remanent magnetization (AIRM) was used in this study, since isothermal remanence gives the largest signal of any of the remanence methods (Potter, 2004), and preliminary tests on our caprock samples showed that other types of magnetic remanence gave extremely low values. The AIRM technique involves applying a direct field (DF) successively along the x, y, and z orthogonal sample reference axes (see Figure 2) and measuring the three components of remanence acquired after each field application ($M_{1x}$, $M_{1y}$, $M_{1z}$ after a field applied along x *etc*). For AIRM this involves applying a pulsed DF (about 100 ms), which we generated using a Molspin pulse magnetizer. The procedure produces nine components of remanence as shown in Equation (1) below:

| Field Axis | Measured Remanence | |
|---|---|---|
| x | $M_{1x}$ $M_{1y}$ $M_{1z}$ | |
| y | $M_{2x}$ $M_{2y}$ $M_{2z}$ | (1) |
| z | $M_{3x}$ $M_{3y}$ $M_{3z}$ | |

These coefficients are then used to compute the 3D anisotropy (Potter, 2004) comprising the magnitude and direction of the three principal anisotropy axes (max, int, min). The sample is tumble alternating field (AF) demagnetized between each DF application. Any residual remanence components in the demagnetized state are subtracted from the subsequent isothermal remanence that is acquired. AMR techniques do not depend on the domain state of the remanence carrying particles (unlike AMS). Single domain and multidomain particles have a maximum remanence along their long axis (Potter, 2004).

**5. Permeability Anisotropy**

In the present study we only had horizontal and vertical core plugs from the same interval, and so the permeability anisotropy was estimated merely from the ratio of the permeability values from the two plugs. The permeabilities were measured via a steady state method using nitrogen gas and were Klinkenberg corrected.

## RESULTS AND DISCUSSION

X-ray diffraction revealed that the main minerals in the horizontal core plug 4H were quartz, muscovite, kaolinite, orthoclase and albite. The visible petrofabric in plug 4H (shown mainly by the alignment of muscovite grains using a hand lens and in thin sections) was closely parallel to the y and z axes (green and red arrows in Figure 2) and closely perpendicular to the x axis (blue arrow in Figure 2). X-ray diffraction revealed that the main minerals in the vertical core plug 2V were quartz, muscovite, kaolinite, sanidine and albite. The visible petrofabric in plug 2V (shown again mainly by the alignment of muscovite grains) was closely parallel to the x and y axes (blue and green arrows in Figure 2) and closely perpendicular to the z axis (red arrow in Figure 2).

Figure 3 shows the *p*-wave velocities with applied hydrostatic pressure during the up cycle along the long axis (z axis) of the horizontal plug 4H and vertical plug 2V. The

uncertainties in the measurements are smaller than the symbol size. The *p*-wave in plug 4H is closely parallel to the observed petrofabric and the velocity is higher than for plug 2V (as expected), where the *p*-wave is closely perpendicular to the petrofabric. The ratio of the parallel to perpendicular *p*-wave velocity at 40 MPa is 1.084 ± 0.005.

Figure 4 shows the *s*-wave velocities with applied hydrostatic pressure during the up cycle along the x and y axes of the horizontal plug 4H. The *s*-wave velocity is higher along the y-axis than along the x-axis. The y-axis is quite close to being parallel to the petrofabric and the x-axis close to being perpendicular to the petrofabric. We also measured the *s*-wave velocities as close as possible parallel and perpendicular to the petrofabric of the same plug 4H using our own observations of the petrofabric (rather than along the x, y and z sample axes labelled by the company who supplied the plugs). We did this by visually orienting the plug from a series of quasi-parallel lines (which indicated the petrofabric and was due mainly to the alignment of the mica grains) using a hand lens on the end faces of the plug, and arranging the s-wave transducers to polarize the *s*-waves parallel and perpendicular to those mineral alignment lines. The results are shown in Figure 5, together with the results along the x and y axes for comparison. There are small differences between the two sets of results, with the measurements along our estimated axes parallel and perpendicular to the petrofabric showing a slightly greater anisotropy. The ratio of the parallel to perpendicular *s*-wave velocity at 40 MPa is 1.061 ± 0.005.

Figure 6 shows the *s*-wave velocities with applied hydrostatic pressure during the up cycle along the x and y axes of the vertical plug 2V. In this plug both the x and y axes are in the plane essentially parallel to the petrofabric. The acoustic results are consistent, since there is little difference (particularly at higher pressures) between the *s*-wave velocities along the x and y axes in this plug.

Table 1 shows the anisotropy of magnetic susceptibility (AMS) results for the vertical plug 2V with respect to the x, y and z sample reference axes (the x axis would have a declination and inclination of 0 degrees, the y axis would have a declination of 90 degrees and inclination of 0 degrees, and the z axis would have a declination of 0 degrees and inclination of 90 degrees). The key result is that the maximum axis for plug 2V is in the horizontal plane (shown by the low inclination value). This is consistent with the observed petrofabric. The AMS results indicate that the magnetic fabric is slightly planar with the maximum and intermediate normalised axes (0.354 and 0.337) being closer in magnitude and significantly different from the normalised magnitude of the minimum axis (0.309). The results are generally consistent with the observed petrofabric. Table 2 shows the anisotropy of isothermal remanent magnetization (AIRM) results acquired in a DF of 80mT. This shows that the remanence carrying particles (mainly ferrimagnetic iron oxides) are also aligned in a slightly planar way (the normalised maximum and intermediate axes, 0.362 and 0.339, are closer in magnitude and there is a larger difference between these and the normalised magnitude of the minimum axis, 0.299). The inclination values of the maximum and intermediate axes show that the plane is just a few

degrees away from the horizontal, and the minimum axis has a steep inclination. This is all consistent with the observed petrofabric in this plug. However, the absolute IRM magnitudes were extremely low, indicating very small amounts of the ferrimagnetic particles (a few ppm). Table 3 shows the anisotropy of magnetic susceptibility (AMS) results for the horizontal plug 4H. In this plug the observed petrofabric lies roughly in the zy plane. Therefore one might expect the maximum and intermediate AMS axes to be close to this plane. The intermediate AMS axis is reasonably close to the y axis, and the maximum AMS axis has a fairly high inclination but not as high as the z axis. The AMS results may not exactly mimic the observed petrofabric because (i) the absolute values of magnetic susceptibility were very low and small uncertainties in the magnitudes can significantly affect the orientation data, and (ii) the observed petrofabric varies slightly along the 4H plug (Figures 1 and 2) and the AMS measurements were taken from one section of the plug (Figure 1). Likewise the AIRM results for plug 4H (Table 4) may not be representative of the observed petrofabric partly due to point (ii) above, and also because the IRM values were extremely low for this plug, indicating an extremely low concentration of ferrimagnetic particles.

Plug permeability measurements on the same core material gave Klinkenberg corrected values of 0.04 mD for the horizontal plug 4H and 0.03 mD for the vertical plug 2V. The uncertainties in these values are estimated to be ± 0.005 mD. Table 5 gives a comparative summary of the anisotropies determined from all the quantitative methods.

## CONCLUSIONS

1. The acoustic *p*-wave velocity was greater in the horizontal plug 4H (parallel to the visible petrofabric) than the vertical plug 2V (perpendicular to the visible petrofabric).
2. Acoustic *s*-wave velocity measurements along the x and y axes of the horizontal plug 4H exhibited a higher velocity along the y axis (closely parallel to the visible petrofabric) than along the x axis (closely perpendicular to the visible petrofabric). Further *s*-wave velocity measurements parallel and perpendicular to the observed petrofabric (using our own observations of the petrofabric) showed an even larger difference between the two velocities, with the parallel velocity again being larger.
3. Acoustic *s*-wave velocity measurements along the x and y axes of the vertical plug 2V were very similar, consistent with both these axes being closely parallel to the visible petrofabric in this plug.
4. Low field anisotropy of magnetic susceptibility (AMS) for the horizontal and vertical plugs were consistent with the acoustic anisotropy and visible petrofabric in these two samples.
5. The anisotropy of isothermal remanent magnetization (AIRM) results for the vertical plug 2V were consistent with the results for the other anisotropy techniques, indicating that the ferrimagnetic particles were also approximately aligned in the same orientation as the overall petrofabric. The magnitude of the IRM for plug 4H was too low to give meaningful results regarding the orientations of the AIRM rincipal axes.

6. The large signal (particularly at reservoir pressures) and low measurement uncertainties in the *p*- and *s*-wave acoustic data demonstrated that there is a definite anisotropy between the horizontal and vertical directions in the caprock samples studied. The magnetic anisotropy data also suggested an anisotropy that was consistent with the acoustic results, although the low magnetic signal in some cases (particularly for the AIRM of plug 4H) made this difficult to ascertain. Whilst the permeability was also higher in the horizontal plug than the vertical plug, the larger measurement uncertainties meant that it was difficult to tell from the permeability data alone whether the anisotropy was real.
7. The observed acoustic and magnetic anisotropies would suggest that the permeability anisotropy is real, with a lower vertical permeability than horizontal permeability. The anisotropic nature of these samples would seem to be one factor in making this an efficient caprock, even though the permeability values are larger than one might expect for a traditional caprock. Further acoustic and magnetic anisotropy studies on other caprock samples may be useful in assessing the efficiency of each caprock.

## ACKNOWLEDGEMENTS

We thank Wintershall Norge and Weatherford Laboratories for supplying core material and other supplementary data.

## REFERENCES

Bakhorji, A. M., 2010. Laboratory measurements of static and dynamic elastic properties in carbonates. PhD thesis, Department of Physics, University of Alberta.

Hemsing, B. D., 2007. Laboratory determination of seismic anisotropy in sedimentary rock from the Western Canadian Sedimentary Basin. M.Sc. thesis, Department of Physics, University of Alberta.

Potter, D. K., 2004. A comparison of anisotropy of magnetic remanence methods - a user's guide for application to palaeomagnetism and magnetic fabric studies. Geological Society, London, Special Publications, **238**, 21-35.

**Table 1.** Table showing AMS principal anisotropy axes, normalised magnitudes, declination and inclination values for sample 2V (vertical plug).

| Method | Principal Anisotropy Axes | Normalised magnitudes | Directions (with respect to the x, y and z sample axes) | |
|---|---|---|---|---|
| | | | Declination | Inclination |
| Low field AMS | Maximum | 0.354 | 29.7 | 0.3 |
| | Intermediate | 0.337 | 299.1 | 64.1 |
| | Minimum | 0.309 | 119.8 | 25.9 |

**Table 2.** Table showing AIRM principal anisotropy axes, normalized magnitudes, declination and inclination values for sample 2V (vertical plug).

| Method | Principal Anisotropy Axes | Normalised magnitudes | Directions (with respect to the x, y and z sample axes) | |
|---|---|---|---|---|
| | | | Declination | Inclination |
| IRM at DF 80mT | Maximum | 0.362 | 347.5 | 14.1 |
| | Intermediate | 0.339 | 249.8 | 28.3 |
| | Minimum | 0.299 | 101.0 | 57.8 |

**Table 3.** Table showing AMS principal anisotropy axes, normalised magnitudes, declination and inclination values for sample 4H (horizontal plug).

| Method | Principal Anisotropy Axes | Normalised magnitudes | Directions (with respect to the x, y and z sample axes) | |
|---|---|---|---|---|
| | | | Declination | Inclination |
| Low Field AMS | Maximum | 0.338 | 222.4 | -48.0 |
| | Intermediate | 0.333 | 109.1 | -19.6 |
| | Minimum | 0.329 | 4.4 | -35.3 |

**Table 4.** Table showing AIRM principal anisotropy axes, normalized magnitudes, declination and inclination values for sample 4H (horizontal plug).

| Method | Principal Anisotropy Axes | Normalised magnitudes | Directions (with respect to the x, y and z sample axes) | |
|---|---|---|---|---|
| | | | Declination | Inclination |
| IRM at DF 80mT | Maximum | 0.364 | 2.7 | 14.9 |
| | Intermediate | 0.326 | 262.7 | 33.2 |
| | Minimum | 0.309 | 113.3 | 52.8 |

**Table 5.** Summary comparative table showing acoustic and permeability anisotropy ratios, magnetic anisotropy ratios, and full 3D AMS and AIRM anisotropies for the horizontal (4H) and vertical (2V) plugs.

| **Acoustic & Permeability Ratios (Parallel / Perpendicular to Petrofabric)** | |
|---|---|
| ***p*-wave velocity at 40 MPa (up cycle)** | 1.084 ± 0.005 (using plugs 4H and 2V) |
| ***s*-wave velocity at 40 MPa (up cycle)** | 1.061 ± 0.005 (using plug 4H) |
| **Permeability** | 1.3 ± 0.4 (using plugs 4H and 2V) |

| **Magnetic Anisotropy Ratios (Maximum / Minimum)** | | |
|---|---|---|
| **AMS** | 4H (Horizontal plug) | 1.027 ± 0.001 |
| | 2V (Vertical plug) | 1.146 ± 0.001 |
| **AIRM** | 4H (Horizontal plug) | 1.18 ± 0.01 |
| | 2V (Vertical plug) | 1.210 ± 0.002 |

| | ***AMS %** | ***AIRM %** |
|---|---|---|
| 4H (Horizontal plug) | 0.90 ± 0.01 | 5.5 ± 0.4 |
| 2V (Vertical plug) | 4.50 ± 0.04 | 6.3 ± 0.1 |

*AMS and AIRM percentages refer to 100 (max – min)/total.

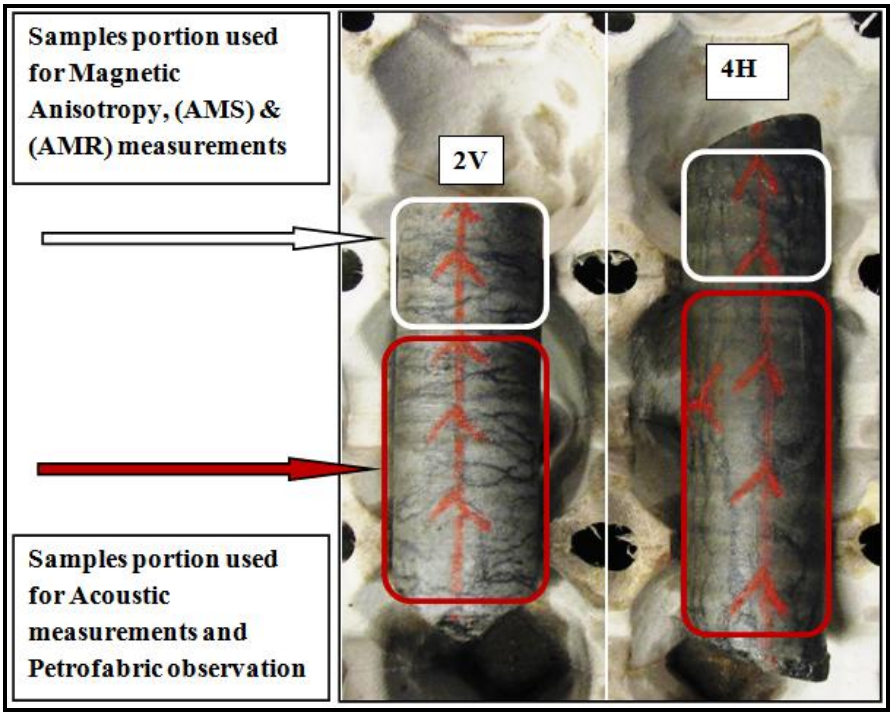


**Figure 1.** Images of the vertical (2V) and horizontal (4H) caprock core plugs, showing the portion of each plug that was used for acoustic anisotropy, magnetic anisotropy and visible petrofabric analysis.

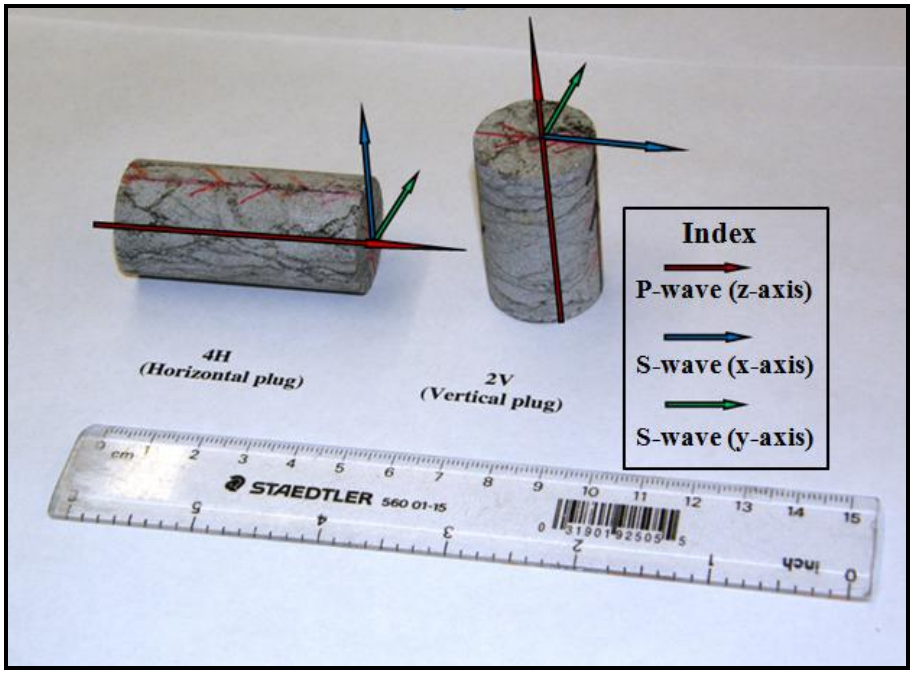


**Figure 2.** Photograph showing the orthogonal axes along which *p*- and *s*-waves were measured. The y and z axes in plug 4H are closely parallel to petrofabric, while in plug 2V the x and y axes are closely parallel to petrofabric. The x axis in plug 4H and the z axis in plug 2V are closely perpendicular to petrofabric.

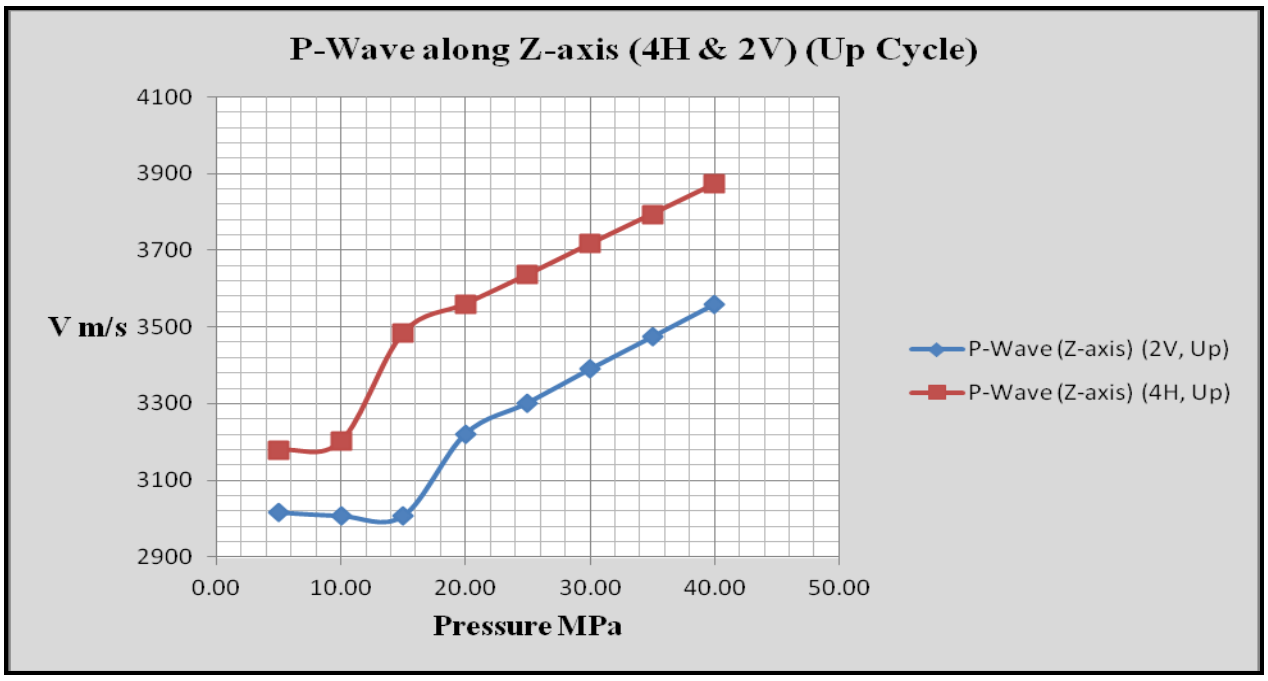


**Figure 3.** *p*-wave velocity with pressure (up cycle) along the z axes of horizontal plug 4H and vertical plug 2V. In plug 4H the z axis is closely parallel to petrofabric, whilst in plug 2V the z axis is closely perpendicular to petrofabric.

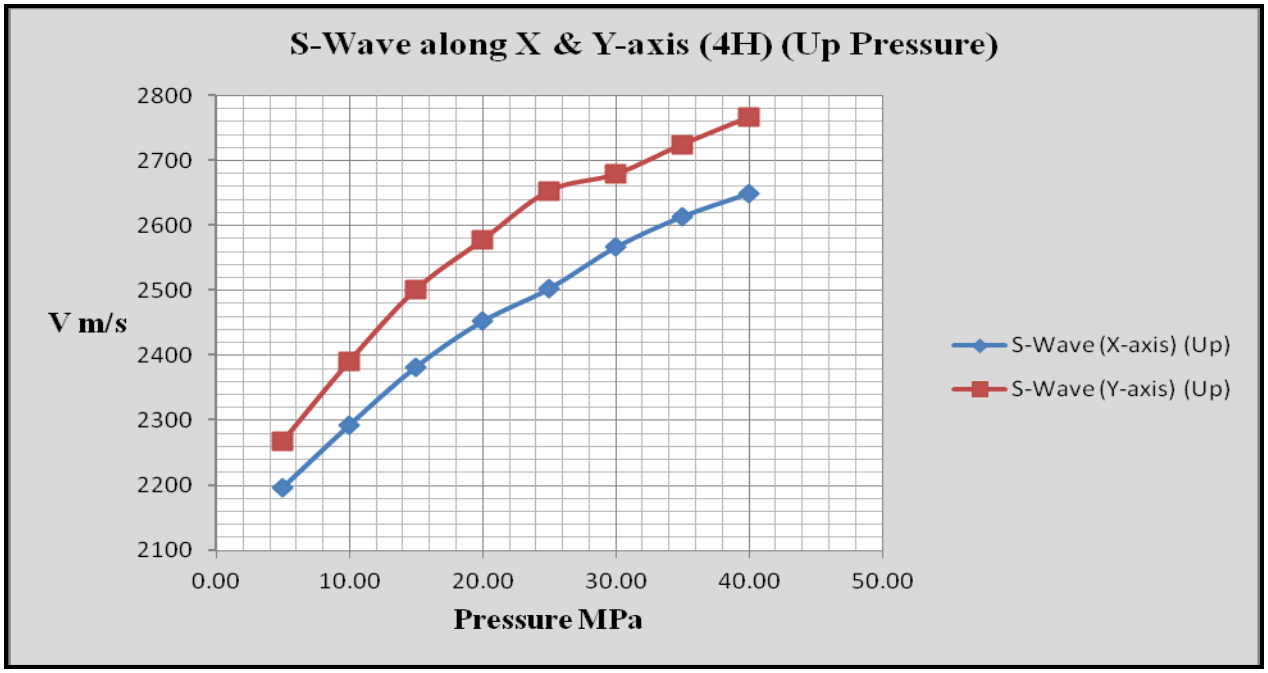


**Figure 4.** *s*-wave velocity with pressure (up cycle) along the x and y axes of horizontal plug 4H. The y axis is closely parallel to the petrofabric, whilst the x axis is closely perpendicular to the petrofabric.

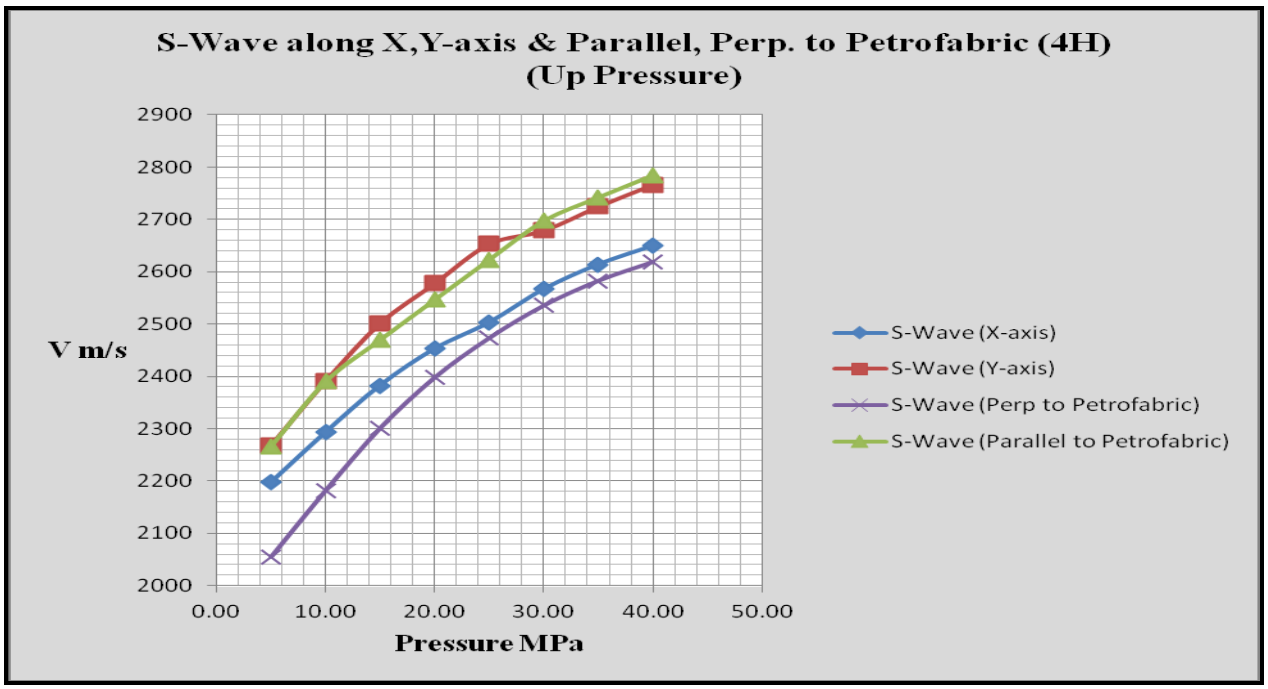


**Figure 5.** *s*-wave velocity with pressure (up cycle) parallel and perpendicular to petrofabric based on our observations of the petrofabric for horizontal plug 4H. The results are also compared with the results along the x and y axes (which were labelled by the company who supplied the plugs) as shown in Figure 5.

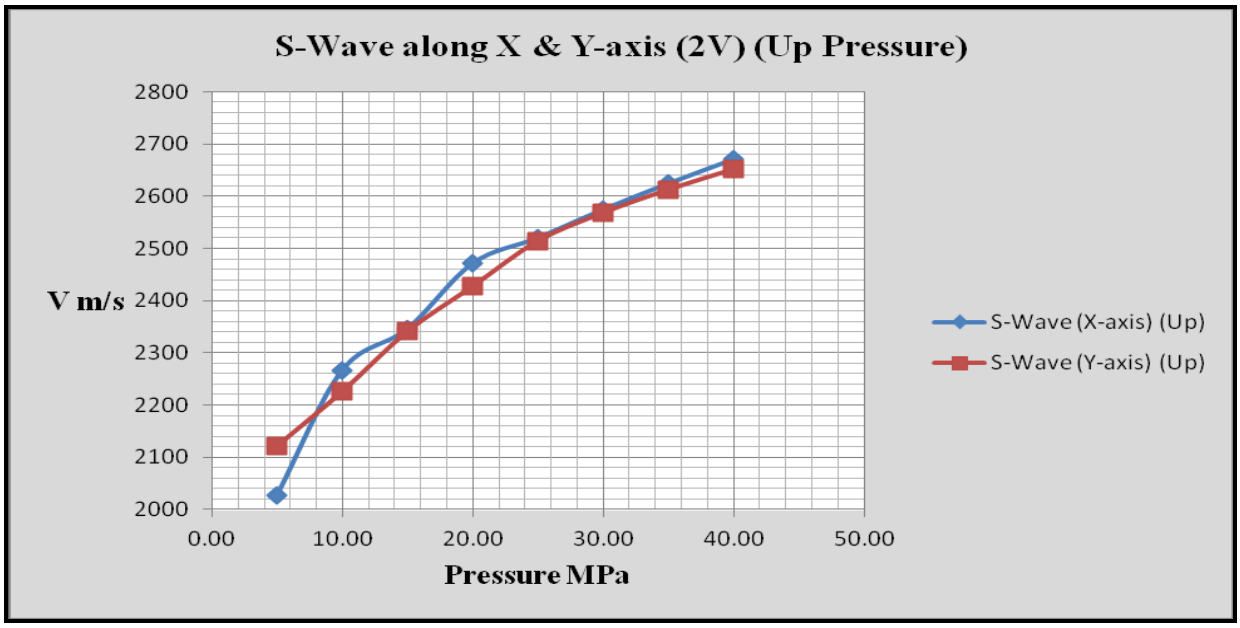


**Figure 6.** *s*-wave velocity with pressure (up cycle) along the x and y axes of vertical plug 2V. The x and y axes are both closely parallel to the petrofabric in this case.